20th IMEKO TC4 International Symposium and
18th International Workshop on ADC Modelling and Testing
Research on Electric and Electronic Measurement for the Economic Upturn
Benevento, Italy, September 15-17, 2014

Design of a bitonal dielectric resonator for the measurement of anisotropic surface impedance

N. Pompeo[1,2], K. Torokhtii[1], E. Silva[1]

[1]*Dept. of Engineering, Università Roma Tre, Via della Vasca Navale 84, Rome, Italy*
[2]*nicola.pompeo@uniroma3.it*

***Abstract* – The measurement of the microwave surface impedance is a fundamental characterization tool for a wide class of conducting, semiconducting and superconducting materials. In many cases, material anisotropy can show up as an intrinsic or tailored property, and its measure is often desirable. Microwave resonators can be designed to give at the same time non-destructive and highly sensitive measurements, in particular with the surface perturbation method for planar samples. Rectangular resonators can be designed to preserve sensitivity to the anisotropy of the samples under study, since they can induce straight currents on the sample. In this manuscript we report on the design, based on finite elements electromagnetic simulations, of a rectangular dielectric resonator which induces straight currents on the sample, with the additional feature of simultaneous operation at two different resonant frequencies, to allow multifrequency study e.g., for validation of the results.**

I. INTRODUCTION

Microwave measurements have been for long a powerful and widespread tool to study the conductivity and the electric permittivity of various classes of materials (including but not limited to dielectrics, semiconductors, (super)conductors), for both technological applications [1] and basic material science [1]. Resonant techniques, although limited to fixed frequencies, exhibit high sensitivity [2], are non-destructive (do not require sample patterning) and contactless: all are positive features. Within a perturbation approach, the sample to be measured is placed either inside the volume of the resonator or as part of its conducting enclosing surface [3]. For each electromagnetic mode, by measuring the variations of the resonator quality factor Q and resonant frequency f_{res} due to the insertion of the sample, one extracts the sample properties with a sensitivity which is essentially dictated by Q (the higher, the better) [2, 4]. Typical measurement applications are the contactless determination of the conductivity of semiconductors [1], including resistance mapping, in the integrated electronics industry; the characterization of dielectric materials for electronics and telecommunications [5]; the study of the photoconductivity in insulating materials to be used in scintillators, phosfors for fluorescent tubes and plasma panels [6]; the study of the complex impedance of superconductors [7].

The physical quantity which is measured through the microwave resonant techniques is the surface impedance Z_s. Considering an electromagnetic field incident on a flat interface between air/vacuum and a conductor, the surface impedance is defined [8] as $Z_s = E_{//}/H_{//}$, where $E_{//}$ and $H_{//}$ are the components of the electric and magnetic field parallel to the surface, respectively. In the case of semi-infinite conducting material, the electromagnetic field decays exponentially with a length scale given by the skin depth $\delta = \sqrt{\omega\mu_0\sigma/2}$, where ω is the angular frequency of electromagnetic field, μ_0 is the magnetic permeability of vacuum and σ is the conductivity (eventually complex). Hence, in the local limit Z_s is given by the well known expression [8]:

$$Z_s = R_s + \mathrm{i}X_s = \sqrt{\frac{\mathrm{i}\omega\mu_0}{\sigma}} \qquad (1)$$

where R_s and X_s are the surface resistance and reactance, which account for dissipation and energy storage, respectively. In thin films the electromagnetic field propagates through the film reaching the underlying substrate and the supporting backplate. Correspondingly, the measured surface impedance is written down through standard impedance transformation expressions [8]. In the common situation in which the film thickness $d \ll \delta$, the so-called thin film approximation [9] applies yielding $Z_s = 1/(\sigma d)$. Once placed inside the resonator in the volume or surface perturbation approach, the sample contributes to the resonator dissipation and energy storage. Its surface impedance Z_s can be then obtained from the measured Q and f_{res} as [8]:

$$\frac{1}{Q} - \mathrm{i}2\frac{\Delta f_{res}}{f_{res}} = \frac{R_s}{G_s} + \mathrm{i}\frac{\Delta X_s}{G_s} + background \qquad (2)$$

where $\Delta X = X(x) - X(x_{ref})$ is a variation with respect to a reference value when a physical parameter x, like temperature or dc magnetic field, is varied. The geometrical factor G_s, related to the volume or surface occupied by the sample, is obtained through electromagnetic computations or, when available, closed formulas. The term "background" represents the resonator contributions, which in most cases have to be experimentally determined,

ISBN-14: 978-92-990073-2-7

and must be subtracted to isolate the sample Z_s. For the special case of the study of anisotropic materials, the rectangular resonators have the correct symmetry to induce straight currents on the sample. In a previous work [10] we have presented the design, realization and characterization of a prototype rectangular rutile (TiO_2) resonator, which gave promising results. Rutile was chosen because of its high dielectric constant, which allowed the design of a very compact resonator. On the other hand, rutile is also an anisotropic dielectric material so that its characterization, the design process and the identification of the resonant modes require a larger effort as compared to isotropic dielectrics.

In this work we study the feasibility of a rectangular microwave resonator based upon an isotropic dielectric prism, with the additional advantage of a two-frequency (bitonal) operation. The latter feature would provide a second, independent measurement of the surface impedance, that can be used either for validation of the results or for the determination of frequency-dependent features.

In the following Sections, we report on the design process, based on finite elements electromagnetic simulations, of the resonator under development: in Section ii. we recall the main design goals and principles; in Section iii. we present the results of the simulations for the bitonal resonator (iii.A.), including the evaluation of the effects of a low-loss gap in the fine-tuning of the resonator parameters (iii.B.) and estimates of the dynamic range and uncertainties in the measurements of the anisotropy (iii.C.). Short conclusions and perspectives are presented in Section iv..

II. REQUIREMENTS

Rectangular (i.e., prisms in the shape of a parallelepiped) dielectric resonators (RDR) are commonly used as radiative elements for the realization of miniaturized antennas. For this very reason, these devices are optimized for efficient radiation, and as a consequence they present several open ended faces (OEF). This is quite contrary to the needs of a measuring device, where one needs to concentrate the electromagnetic fields in the volume of the device itself in order to raise sensitivity. Thus, most of the design procedure available for rectangular resonators cannot be directly employed.

In a previous work [10], we have proposed an RDR for the measurement of anisotropic conductive materials based on rutile (TiO_2), a very high permittivity and anisotropic dielectric. The choice allowed for a very compact device, with satisfactory performances, but the anisotropy of rutile added significant complications to the design. Moreover, the high value of the dielectric constant along the rutile anisotropy axis determines an undesired crowding of the spurious modes, making more difficult the selection of two well isolated modes for the bitonal operation planned in the present design. Finally, the Q factor at room temperature

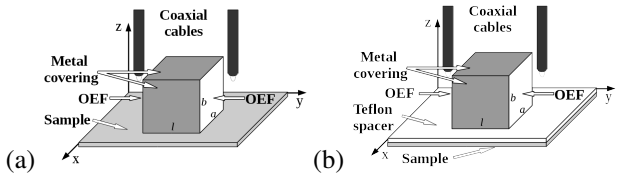

Fig. 1. The configuration of the rectangular dielectric resonator with two open ended faces, without (a) and with (b) a low-loss spacer. Coupling loops are depicted.

was limited by the rather large dielectric losses. Thus, we are led to explore the use of an isotropic dielectric such as $LaAlO_3$. Its dielectric constant $\varepsilon_r(1 + \mathrm{i}\tan\delta)$ depends on the crystal purity [11, 12], but typical reported values are clustered around $\varepsilon_r = 24$, with loss tangent $\tan\delta = 1.3 \cdot 10^{-5}$ at room temperature [11]. The latter decreases down to $\tan\delta = 2.5{\cdot}10^{-6}$ at $T = 77$ K. In the following, we will neglect the dielectric losses, since they are usually lower than the ohmic losses in the configuration that we explore. We will use $\varepsilon_r = 24.5$ as room temperature values, as declared by a crystal producing company [13].

The large value of ε_r reduces the radiation losses, allowing two OEF for the necessary coupling of the resonator to the external lines (measurements in transmission are widely recognized as optimal in terms of performances [14]). Moreover, the dimensions of the device are reduced, and smaller areas can be sensed [10]. OEFs reduce ohmic dissipation on the metallized surfaces, but also reduce the region where the induced currents are straight. As a trade-off, we adopted a design with two OEF for coupling, one face directed toward the sample and three metallized faces, as schematically sketched in Fig. 1. The two OEF allow to operate the resonator in transmission, once inserted in a measurement system such as the one described in Ref. [4]. The resonant mode chosen to ensure straight currents on the sample surface are the TE_{011} and TE_{021} (the subscripts indicate the variation of the electric field along x, z, y, respectively; (x, z) is parallel to the OEFs).

Even in the TE_{011} and TE_{021} modes, the OEFs distort the currents from perfectly straight lines. This effect is relevant in the region of the sample outside of the region covered by the dielectric prism. Since straight currents are required to be sensitive to the anisotropy, we introduce a figure of merit for such a curvature [10] as the parameter $j_{\%} = J_{\mu w,\perp}/J_{\mu w,\parallel}$, where $J_{\mu w,\parallel}$ and $J_{\mu w,\perp}$ are the current densities along the desired direction and perpendicular to it, respectively. Setting a threshold of acceptable deviation at $j_{\%} \sim$ 1-5 %, one obtains the available area for the measurements. The sample area exposed to the microwave field can be selected by using a thin metal mask. In the next Section we perform the simulations of the response of the designed structure, in order to assess the performances with particular emphasis on the sensitivity to the

anisotropy of the sample under study.

III. SIMULATIONS

A. Parameters of the bitonal resonator

Since the present work will be used for a practical realization of the resonator, we have studied the Q an f_{res} of an existing $LaAlO_3$ crystal, with $\varepsilon_r = 24.5$ and dimensions $3.9 \times 3.5 \times 4.5$ mm^3. The resonant frequencies were calculated first following the closed forms for the TE$_{mnp}$ DR modes considering a waveguide partially filled with a dielectric [15]. Secondly, in order to properly take into account the main details of a feasible practical realization, we employed numerical simulations with CST MWS® where, with respect to Fig. 1, we have taken the lower base as infinite. The rectangular mask used to select the straight-current subregion was taken into account in the simulations. It can be seen that both TE$_{011}$ and TE$_{021}$ are well isolated. In particular, all nearby modes can be identified in Fig. 2 at zero Teflon spacing (see below), showing ≈0.45 GHz separation.

The currents are straight, as measured by the $j_{\%}$ parameter introduced in the previous Section: by setting an acceptable threshold of $j_{\%} = 5\%$, one obtains 100% and 98% of the area under the RDR for the TE$_{011}$ and TE$_{021}$ modes, respectively.

B. Effects of a low-losses spacer

It has been suggested [16] and experimentally confirmed [10, 16] that the introduction of low-losses spacers gives a reduction of ohmic losses, with a consequent increase of the Q-factor, and a controllable variation of the resonant frequencies of the modes. Both features are particularly useful, but are contrasted by a reduction of the region of the sample where $J_{\mu w}$ are straight. Thus, it is useful to present here a study of the effect of a thin Teflon spacer between the sample and the RDR.

In order to make contact to practical realizations, in the numerical simulations we consider a geometry with the gap provided by a Teflon low-loss spacer ($\varepsilon_r^* \simeq 2.04$), interposed between the sample surface and the entire resonator assembly (dielectric prism and metal casing), as depicted in Fig. 1b. Given the practical relevance of this geometry, in Fig. 2 we report in Fig.2a a full mode chart up to 19 GHz as a function of the Teflon spacer thickness h, as determined by numerical simulations. In Fig.2b we report the calculated Q factor vs. the Teflon thickness for modes of interest. For what concerns the TE$_{011}$ mode, the spacer thickness h can be increased up to a maximum of 0.2 mm before interference with other modes arises. With this value of h, Q increases from 1590 up to 2345. The TE$_{021}$ mode is free from interference for thicknesses between 0.025 and 0.25 mm, with an increase of Q up to 2830. For the best compromise in terms of Q and frequency spacing, one should choose 0.10 mm $\leq h \leq$ 0.15 mm. For practical construction of the device, this spacer configuration eliminates the need for the ohmic contact between the metal enclosure and the sample, thus simplifying the resonator assembly. On the other hand, the spacer reduces the useful area in which straight currents can be obtained: in Fig. 3 we report the result of the numerical simulations yielding the normalized area where $j_{\%}$ is less than 5%, as a function of the Teflon gap thickness for selected modes. Summarizing, depending on the size of the sample to be measured, one can select the proper spacer thickness between 0 up to ≈ 0.15 mm in order to optimize the Q factor, the exposed sample area and the frequency separation between the desired modes and other modes: the spacer gives a relatively simple method to fine-tune the features of the device.

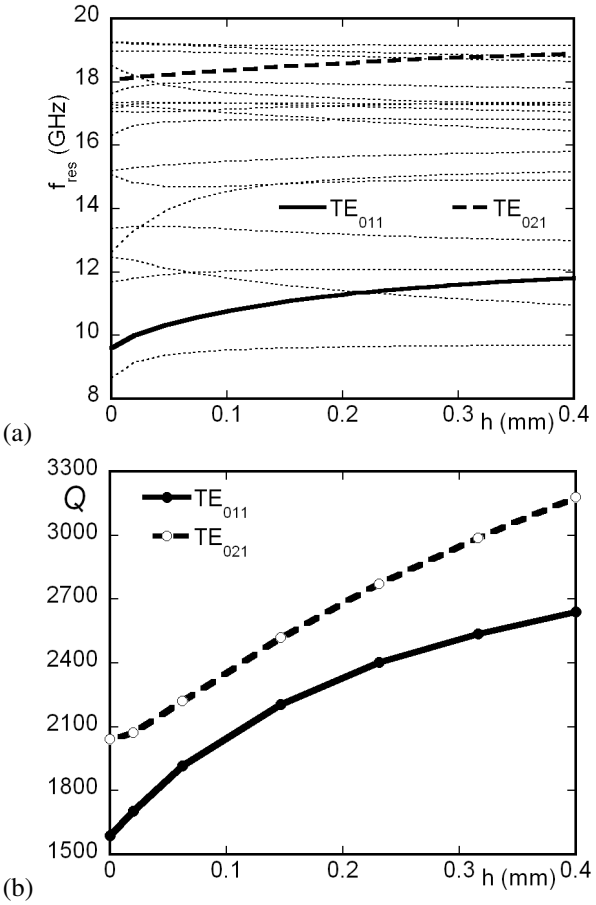

Fig. 2. (a) Mode chart for modes up to 19 GHz vs Teflon spacer thickness. (b) Dependence of the Q factor on the Teflon thickness of the modes of interest.

C. Evaluation of measurement uncertainties

We now study the expected uncertainties in the anisotropy measurements obtainable through the pro-

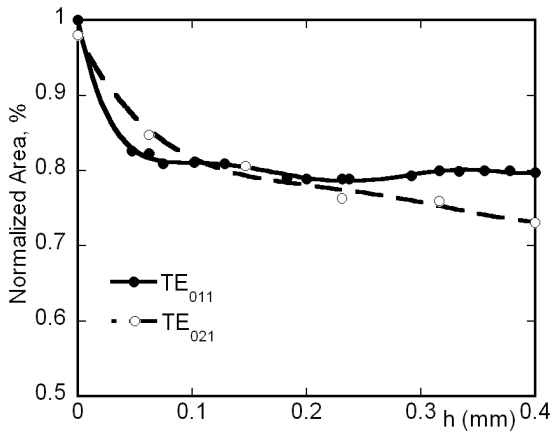

Fig. 3. Percentage of the area below the RDR where currents are straight within $j_{\%} = 5\%$, as a function of the Teflon gap thickness for selected modes.

posed device. Given a sample with a surface resistance anisotropy ratio $\gamma = R_c/R_a \geq 1$ (a and c are in-plane, perpendicular directions), the anisotropy is determined by means of two independent measurements in which the sample is mounted with the probing currents parallel and normal to the direction a. By denoting with $Q_{\parallel}$ and $Q_{\perp}$ the corresponding Q factors, one obtains:

$$\frac{1}{Q_{\parallel}} = \frac{R_a}{G_s}(p_{\parallel} + \gamma p_{\perp}) + \frac{1}{Q'} \quad (3)$$

$$\frac{1}{Q_{\perp}} = \frac{R_a}{G_s}(\gamma p_{\parallel} + p_{\perp}) + \frac{1}{Q'} \quad (4)$$

where Q' represent the resonator contribution to losses, and $p_{\parallel}$ and $p_{\perp}$ are normalized coefficients ($p_{\parallel} + p_{\perp} = 1$) measuring the relative weight of the straight and transverse currents $J_{\mu w,\parallel}$ and $J_{\mu w,\perp}$. An approximate, worst-case evaluation yields $p_{\perp} < 0.5 j_{\%}^2$, so that by setting $j_{\%} \sim 5\%$ one can neglect the terms with $p_{\perp}$ for $\gamma < 800$. Solving the above equations for γ one obtains:

$$\gamma = \left(\frac{1}{Q_{\parallel}} - \frac{1}{Q'}\right) / \left(\frac{1}{Q_{\perp}} - \frac{1}{Q'}\right) \quad (5)$$

For the TE_{011} and TE_{021} modes, the simulations yield similar geometrical factors ($G_s \simeq 300$ and $\simeq 400$, respectively) and similar $Q_{max} \sim 2000$, so that the following holds for both of them. The relatively low values of Q, typical of the rectangular structures, allows to neglect the dielectric with respect to ohmic losses; moreover, the main source of uncertainty is the Q itself, whereas the uncertainties on the various geometrical factor can be safely ignored (neglecting, for now, centering and position mechanical issues). The relative uncertainty $\delta\gamma/\gamma \approx 3\delta Q/Q$ with a typical error $\delta Q \approx 10$ and $Q_{max} \sim 2000$ (see Ref. [4] for a discussion and more bibliographic references about the uncertainty on the Q factor), yields in the best case $\delta\gamma/\gamma \sim 1.5\%$. The dynamic of the measurements of γ can be estimated as follows. The maximum measurable anisotropy is related to the ratio between the minimum measurable R_a and the maximum measurable R_c. The minimum measurable R_a is determined by the system sensitivity $S = \partial Q/\partial R_s = Q^2/G_s$ [4], $R_{a,min} \sim S^{-1}\delta Q$. The maximum measurable R_c is determined by the minimum measurable $Q \sim 100$, corresponding in the present case to $R_c \sim 3 \div 4\ \Omega$. By accepting a relative uncertainty of 10% for the minimum resistance sensed, one can expect to measure a maximum anisotropy ~ 400. It is worth noting that the better mode isolation achievable with the lower dielectric constant of $LaAlO_3$ with respect to rutile is beneficial also in estending the dynamics range of the device, allowing to measure lower Q factors (which require a larger frequency window devoid of spurious modes), and therefore higher R_c. Hence, with the minimum R_a limited by the device sensitivity, the higher measurable R_c translates to higher measurable anisotropy ratios.

IV. CONCLUSIONS

Summarizing, we have studied a dielectric resonator, based on the high permittivity isotropic $LaAlO_3$, as a device for the measurement of the surface impedance in anisotropic materials. The rectangular prism shape and appropriate microwave modes were chosen in order to generate straight microwave currents. Extensive numerical simulations were performed to design the resonator and study the effects of different spacers, intended to fine-tune resonator properties such as Q factors, resonant frequencies and current straightness. We defined a design which enables the simultaneous use of two resonant modes, thus allowing multifrequency measurements in the same measurement session.

REFERENCES

[1] J.Krupka, "Contactless methods of conductivity and sheet resistance measurement for semiconductors, conductors and superconductors", Meas. Sci. Technol., vol.24, 2013, pp.062001.

[2] J.Mazierska, C.Wilker, "Accuracy Issues in Surface Resistance Measurements of High Temperature Superconductors Using Dielectric Resonators (Corrected)", IEEE Trans. App. Supercond., vol.11, 2001, pp.4140–4147.

[3] L.F.Chen, C.K.Ong, C.P.Neo, V.V.Varadan, V.K.Varadan, "Microwave Electronics: Measurement and Materials Characterization", John Wiley & Sons, Ltd, 2004.

[4] N.Pompeo, K.Torokhtii, E.Silva, "Dielectric Resonators for the Measurements of the Surface Impedance of Superconducting Films", Meas. Sci. Rev., vol.4, 2014, pp.164–170.

[5] J.Krupka, "Frequency domain complex permittivity

measurements at microwave frequencies", Meas. Sci. Technol., vol.17, 2006, pp.R55–R70.

[6] H.Loudyi, Y.Guyot, S.A.Kazanskii, J.-C.Gâcon, C.Pédrini, M.-F.Joubert, "What may be expected from the microwave resonant cavity technique applied to rare-earth-doped insulating materials?", Phys. Stat. Sol. (C), vol.4, 2007, pp.784–788.

[7] Maeda, A., Kitano, H., Inoue, R.,"Microwave conductivities of high-T_c oxide superconductors and related materials", *J. Phys.: Condens. Matter* , vol.17, 2005, pp.R143–R185.

[8] R.E.Collin, "Foundation for Microwave Engineering", McGraw-Hill International Editions, 1998.

[9] S.Sridhar "Microwave response of thin-film superconductors", J. Appl. Phys., vol.63, January 1988, pp.159–166.

[10] K.Torokhtii, N.Pompeo, E.Silva, "A rectangular dielectric resonator for measurements of the anisotropic microwave properties in planar conductors", Meas. Sci. Technol., vol.25, 2014, pp.025601-1–7.

[11] C.Zuccaro, M.Winter, N.Klein, K.Urban, Introduction, "Microwave absorption in single crystals of lanthanum aluminate", J. Appl. Phys., vol.82, December 1997, pp.5695–5704.

[12] J.Krupka, R.G.Geyer, M.Kuhn, J.H.Hinken, "Dielectric properties of single crystals of Al2O3, LaAlO3, NdGaO3, SrTiO3, and MgO at cryogenic temperatures", IEEE Trans. Microw. Theory Techn., vol.42, 1994, pp.1886–1890.

[13] www.neyco.fr/pdf/Materials_J_Substrates.pdf.

[14] P. J. Petersan and S. M. Anlage, "Measurement of resonant frequency and quality factor of microwave resonators: Comparison of methods", J. Appl. Phys., vol. 84, September 1998, pp. 3392–3402, .

[15] B. Yu. Kapilevich, Y. Trubekhin, "Waveguide Dielectric Filtering Structures," Moscow, USSR: Radio and Svjaz, 1990 (in Russian).

[16] Y.Kobayashi and S.Tanaka, "Resonant modes of a dielectric rod resonator short-circuited at both ends by parallel conducting plates," IEEE Trans. Microw. Theory Techn., vol.28, October 1980, pp.1077–1085.